photonics

MDPI

Article

Effect of Twisting Phases on Linear–Circular Polarization and Spin–Orbital Angular Momentum Conversions in Tightly Focused Vector and Scalar Beams

Shu-Dan Wu, Khian-Hooi Chew and Rui-Pin Chen *

Key Laboratory of Optical Field Manipulation of Zhejiang Province, Department of Physics, Zhejiang Sci-Tech University, Hangzhou 310018, China
* Correspondence: chenrp@zstu.edu.cn

Abstract: We theoretically investigated the effect of a new type of twisting phase on the polarization dynamics and spin–orbital angular momentum conversion of tightly focused scalar and vector beams. It was found that the existence of twisting phases gives rise to the conversion between the linear and circular polarizations in both scalar and vector beams during focusing. The linear–circular polarization conversion further leads to an optical spin–orbital angular momentum transformation in the longitudinal component (LC). Therefore, even in a scalar optical field with a uniform linear polarization distribution, a circular polarization (spin angular momentum), and an orbital angular momentum (OAM) can appear in the cross-section and the longitudinal component, respectively, while being tightly focused. The novel distributions of the optical field, state of polarization (SOP) and OAM in the focal region are sensitively dependent on the twisted strength of the twisting phase. These results provide a more flexible manipulation of a structured optical field in the aspects of the optical field, SOP, and OAM.

Keywords: twisting phase; vector beams; state of polarization (SOP); orbital angular momentum (OAM)

Citation: Wu, S.-D.; Chew, K.-H.; Chen, R.-P. Effect of Twisting Phases on Linear–Circular Polarization and Spin–Orbital Angular Momentum Conversions in Tightly Focused Vector and Scalar Beams. *Photonics* **2023**, *10*, 151. https://doi.org/10.3390/photonics10020151

Received: 1 January 2023
Revised: 29 January 2023
Accepted: 30 January 2023
Published: 1 February 2023

1. Introduction

The tightly focusing properties of an optical field are extensively studied due to their fundamental interests and potential applications, especially for the vector beam with a non-uniform state of polarization (SOP) in the beam cross-section [1–6]. There are two landmark findings about the tightly focused optical field. Firstly, the spin–orbital angular momentum conversion in the longitudinal component (LC) of a tightly focused circular polarized light [7,8] has found corresponding applications such as particle manipulation [9] and information processing [10]. On the other hand, a strong longitudinal electric field generated in a tightly focused radial vector optical field can be manipulated by the initial SOP distribution [1,6]. The super-diffraction phenomenon based on the LC of a tightly focused radial vector optical field has led to many technology breakthroughs in super-resolution imaging [11,12], optical needle [9,13,14], focal field modulation [15], and optical micro-processing [16].

Recently, the modulation of various spatial phases, including the azimuthal phase [17], radial phase [18], and caustic phase [19] on the vector beam, has generated many novel phenomena and extended the applications of a vector beam [1]. A conventional twisted phase discovered by Simon and Mukunda in 1993 is a secondary phase that exists only in the partially coherent beams and can cause the beam to rotate during transmission with non-separability [20]. The effects of a conventional twisted phase on the beam focusing [21], the orbital angular momentum (OAM) [22], and the propagation properties in the linear medium [23] and non-linear media [24] have been extensively explored. More recently, a new type of twisting phase with an expression consistent with the image dispersion term in the Zernike polynomial has been proposed based on the conventional twisted

phase [25]. The advantage of the new twisting phase over the conventional twisted phase is that it can exist in a fully coherent beam and the rotation angle can be adjusted by the twisting phase [25]. Research on beams carrying the twisting phase is still in its infancy but has found promising applications in optical detection and particle manipulation [26]. As a spatially non-uniform phase distribution, the effect of the new type of twisting phase on a tightly focused vector vortex beam may result in novel phenomena including the polarization conversion and the redistribution of spin angular momentum (SAM) and OAM, especially the manipulation of spin–orbital angular momentum conversion in the LC.

In this work, the effect of a twisting phase on the tightly focused properties of scalar and vector beams is theoretically demonstrated. The distribution characteristics of the optical field, SOP, and OAM of a twisted vector optical field in the focal region are analyzed. Both the SAM and OAM appear in the transverse section at the focal region of the twisted beam, regardless of the scalar or vector beams. In particular, the circular polarization appears in the focal region of a scalar twisted beam with uniform linear polarization due to the linear–circular polarization conversion, leading to an optical spin–orbital angular momentum transformation in the LC during the focusing. The interaction among the twisting phase, vortex, and SOP in a vector vortex beam during focusing induces the novel distributions of SOP, OAM, and optical field in the focal region. These results can extend our understanding of the twisted vector optical field and provide a new approach to manipulate a structured optical field by the twisting phase.

2. Intensity Distribution and SOP of a Twisted Vector Beam in the Focal Region

The vector vortex beams with a twisting phase in the field cross-section in the Cartesian coordinate system can be expressed as [17,27,28]

$$E(\rho,\phi) = e^{i(u\rho^2\cos\phi\sin\phi+n\phi)} \times \left[\cos(m\phi+\phi_0)e_x + e^{i\Delta\phi}\sin(m\phi+\phi_0)e_y\right] \quad (1)$$

where u is the twisted strength of the twisting phase, m is the polarization topological charge number, n is the vortex topological charge number. ρ and ϕ are the parameters that describe the polar radius and azimuthal angle of the initial field in polar coordinates, respectively. e_x and e_y are the unit vectors in the x-direction and y-direction, respectively. The only parameter that determines the initial SOP distribution is the azimuthal angle ϕ. When $\Delta\phi = 0$, the x-directional components are in the same phase as the y-directional components, and the initial SOP of the vector optical field is a locally linear polarization. The directions of the linear polarization in the cross-section of the optical field are determined by the azimuthal angle ϕ. When $m = 1$ with the initial phase $\phi_0 = 0$ or $\pi/2$, the vector optical field described by Equation (1) is the radially or azimuthally polarized field [17,19,27,28] with a twisting phase, respectively. When $m = 0$, the optical field is a scalar linear polarized light field. On the other hand, if $\Delta\phi = \pi/2$, there is a phase difference $\pi/2$ between the x component and the y component, resulting in a hybrid SOP distribution with the linear, elliptical, and circular polarizations located at different positions in the cross-section of the optical field. When $m = 0$ with the initial phase $\phi_0 = -\pi/4$ or $\pi/4$, the vector optical field described by Equation (1) degrades into the right- or left-handed circular polarized fields with twisting phases, respectively.

Based on the Richards and Wolf vectorial diffraction theory [29], the three-dimensional optical fields of the vector optical beam with a twisting phase focused by the high numerical aperture (NA) lens in the focal region are derived in the integral formula as

$$
\begin{aligned}
E(r,\varphi,z) = \; & -\frac{ikf}{2\pi}\int_0^{\alpha}\sin\theta d\theta\int_0^{2\pi}\sqrt{\cos\theta}\cdot\exp(iu\rho^2\cos\phi\sin\phi+in\phi)\times\exp[ik(z\cos\theta+r\sin\theta\cos(\varphi-\phi))] \\
& \times\left\{\left[\cos(m\phi+\phi_0)\cos\phi+e^{i\Delta\phi}\sin(m\phi+\phi_0)\sin\phi\right]\begin{pmatrix}\cos\theta\cos\phi\\ \cos\theta\sin\phi\\ \sin\theta\end{pmatrix}\right. \\
& \left.+\left[e^{i\Delta\phi}\sin(m\phi+\phi_0)\cos\phi-\cos(m\phi+\phi_0)\sin\phi\right]\begin{pmatrix}-\sin\phi\\ \cos\phi\\ 0\end{pmatrix}\right\}d\phi
\end{aligned}
\tag{2}
$$

where $k = 2\pi/\lambda$ is the wave number, λ is the wavelength and f is the focal length of the high NA objective. $\alpha = \arcsin(NA/\eta)$ is the maximal angle describing the ratio of the pupil radius to the beam waist radius determined by the NA of the objective lens, and $NA = 0.9$ in this work. η is the refractive index of the surrounding medium. r is the polar radius, φ and z are the azimuthal angle and longitudinal positions of the observation point in the focal region in the cylindrical coordinate system, as shown in Figure 1.

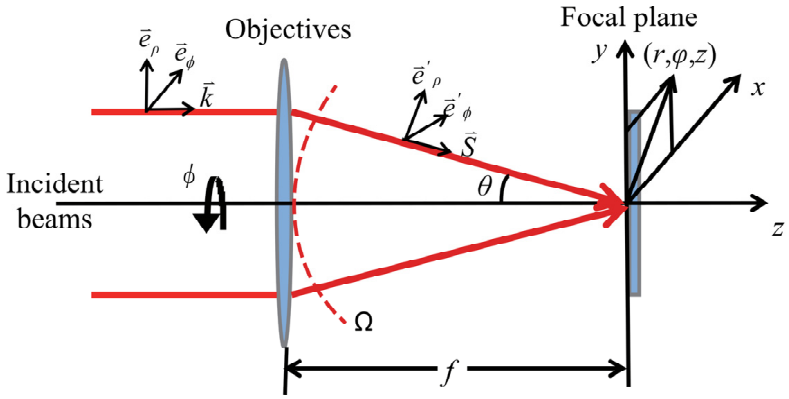

Figure 1. Schematic diagram of a vector vortex beam under a tightly focused condition, where the focal region is located at $z = 0$.

Without the modulation of the twisting phase, the total intensity distribution of a vector beam in the focal region is a petal-like annular spot with $|2m-2|$ petals. In the LC distribution, the number of petal-like annular spots is $|2m-2|$ [30], while in distributions of the transverse x- or y- components, this number equals $|2m|$. In addition, the ring distributions are formed for the focused profiles of the transverse component by combining the x- and y- components, the number of a petal-like annular spots of the total intensity distribution of a vector beam in the focal region is mainly attributed to the contribution of the longitudinal component [31]. However, the effect of the twisting phase on the intensity distribution of the transverse component (TC) and LC of a vector beam in the focal region causes the gradual bending of the $|2m-2|$ petal-like spots and the intensity redistribution in the diagonal (45° and 135°) directions, as shown in Figures 2 and 3. Figure 2 shows the effect of different twisting intensity u on intensity and SOP distributions of a vector beam ($n = 0$, $m = 3$) in the focal region. When the twisted strength $u < 2 \times 10^{12}$ mm^{-2}, the influence of twisting phase on the vortex phase (or polarization topological charge) can be negligible. With the increasing values of twisting strength, the intensity distributions in the diagonal (45° and 135°) directions become obvious with different SOP due to the modulation of the twisting phase. Figure 3 shows the effect of a twisting strength ($u = 10^{13}$ mm^{-2}) on different vector beams in the focal region. The intensity concentration in the diagonal (45° and 135°) directions becomes more evident with the increase in polarization topological charge. In addition, the intensity distributions of different components in the focal region are also sensitively dependent on the modulation of the twisting phase. In particular, the effect of a twisting phase on the tightly focused vector beams with locally linear polarization and hybrid SOP results in the different intensity distributions of the LC, as shown in Figure 3.

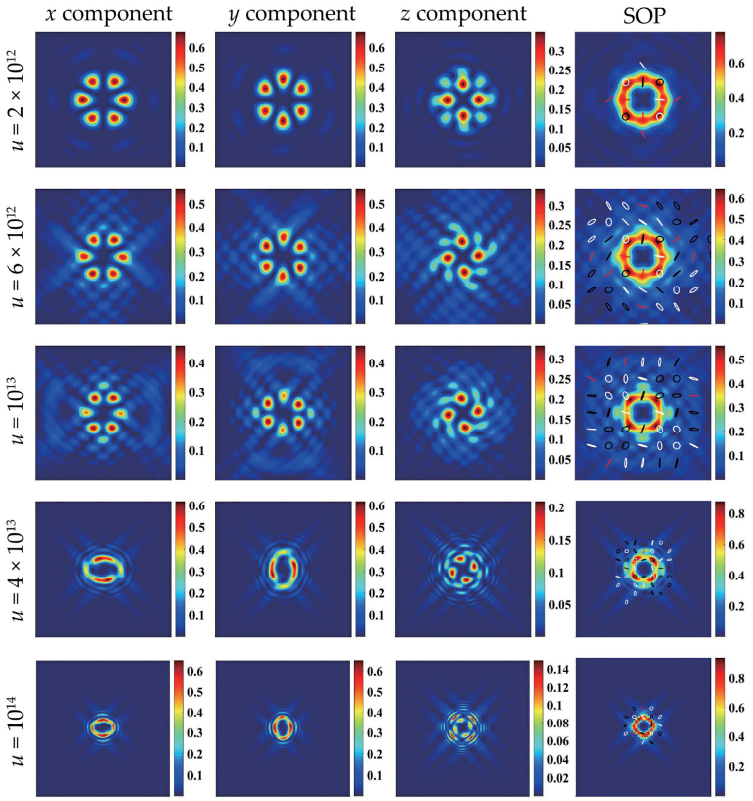

Figure 2. Intensity distributions of the TC (transverse component, x-direction, and y-direction), LC (longitudinal component), and SOP of a vector optical beam ($n = 0$, $m = 3$, $\phi_0 = \pi/2$ in Equation (1)) with different twisted strengths in the focal region. Here the size of each plot is $3\lambda \times 3\lambda$, the red, black, and white lines in the plots in the last column indicate the linear, left-, and right-circular polarizations, respectively.

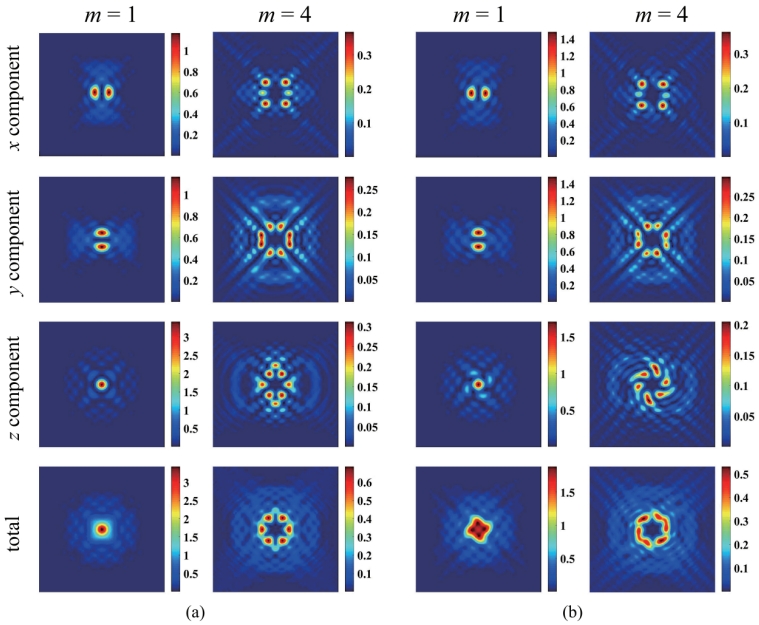

Figure 3. Intensity distributions of the TC (transverse component, x-direction, and y-direction), LC (longitudinal component), and total field of vector optical beams with a twisting phase ($u = 10^{13}$ mm^{-2}) and different polarization topological charges m in the focal region: (**a**) locally linear polarizations ($\Delta\phi = 0$ in Equation (1)); (**b**) hybrid SOP ($\Delta\phi = \pi/2$ in Equation (1)). Here the size of each plot is $3\lambda \times 3\lambda$ and the vortex topological charge $n = 0$.

3. The Effect of a Twisting Phase on Linear–Circular Polarization and SAM-OAM Conversions of the Scalar and Vector Beams in the Focal Region

The linear–circular polarization and SAM-OAM conversions of a structured optical field are important topics in optical field manipulation due to their fundamental interest and practical applications [32–40]. The SAM is dependent on circular polarization [32–34], whereas the OAM is related to the gradient phase distribution [35,36]. The SAM and OAM of a structured beam at the focal region can be calculated as [32–36]

$$S \propto \mathrm{Im}[E^* \times E] \tag{3}$$

$$L \propto \mathrm{Im}[r \times (E^* \cdot (\nabla) E)] \tag{4}$$

where Im[.] represents the imaginary part, and the asterisk denotes the complex conjugate. S and L describe the SAM and OAM densities, respectively. The distributions of SAM at the focal region confirm the occurrence of linear–circular polarization conversion during focusing, as shown in the third column in Figure 4. The appearance and modulation of SAM in the focal region are closely related to the twisting phase and the initial SOP, as a comparison between the first and third columns in Figure 4 shows. In particular, when the initial field is a scalar optical field with a uniform linear polarization distribution, there is a circular polarization appearance in the cross-section in the focal region due to the linear–circular polarization conversion, resulting from the modulation of the spatially non-uniform phase distribution of a twisting phase uxy, as shown in the first row in Figure 4a. If the initial field is a vector optical field with a non-uniform SOP, the conversion of linear–circular polarization gives rise to a novel SOP distribution in the focal region. When the initial SOP is a locally linear polarization ($\Delta\phi = 0$ in Equation (1)), the hybrid polarization state, including linear and circular polarizations, appears with the central symmetry distribution, as shown in Figure 4. If the initial SOP of the optical field is the hybrid polarizations ($\Delta\phi = \pi/2$ in Equation (1)), the SOP distributions of the focused and twisted vector optical field become more complicated because of the linear–circular polarization conversions during propagation. However, the SOP distribution in the focal region retains the central symmetrical shape if the initial SOP is central symmetric, as shown in Figure 4.

The OAM has attracted extensive interest and intensive investigation due to its fundamental interest and applications [35,36]. The spin–orbital angular momentum conversion in LC in the tightly focused circularly polarized scalar optical field has been demonstrated [8,32]. Moreover, the OAM resulting from a twisting phase has been reported [22]. Therefore, the effect of a twisting phase on the optical OAM of a twisted vector beam in the focal region will result in a more complicated spin–orbital angular momentum conversion and redistributions of OAM, especially in the LC.

The optical angular momentum of a structured optical field has been extensively studied in recent years [41–45]. The OAM appears in linearly polarized beams with optical vortices [42–44], in particular, the specific SAM orthogonal to the propagation direction of a linearly polarized vortex beam during propagation [42–45]. Many interesting results about angular momentum have been analyzed and reported such as the spin–orbit interaction [37,38], and the angular momentum of focused beams [39,40]. Different from the vortex phase with a spiral distribution, the twisting phase uxy can compress the optical field in the $\pm 45^\circ$azimuthal angle [46]. The SAM appears in the focal region due to the linear–circular polarization conversion (see the first row in Figure 4a and the first rows in Figure 5a,b), which further results in the appearance of OAM in LC during focusing, as shown in the third rows in Figure 5a,b for the twisting strength $u = 10^{13}$ mm^{-2} and 8×10^{13} mm^{-2}. In addition, the existence of a twisting phase can not only induce the OAM of TC, but also redistributes the OAM of the vortex in the field cross-section, as shown in the second rows in Figure 5a,b. For a scalar optical field with left or right circular polarization, the OAM of the LC and TC in the focused vortex field has been extensively explored [47]. There are no OAM, either for a focused non-vortex with circular polarizations in the TC, or for a focused 1-order vortex ($n = 1$) with the right circular polarization in the LC, as shown

in Figure 6a,b [7]. Interestingly, the OAM appears in both the two cases if the initial field is embedded with a twisting phase, as shown in Figure 6c,d. By comparing Figures 5 and 6, it is evident that even in a scalar field, the influences of the twisting phase on the OAM of the LC are different for linear and circular polarizations. For a scalar vortex beam with circular polarization, both the OAM in TC and LC are affected by the presence of the twisting phase. In particular, they are redistributed in the focal region due to the modulation of the twisting phase, as shown in Figure 6c,d. With the increase in the twisting strength u, the modulation effect of the twisting phase becomes more obvious. The OAM distributions in the diagonal (45° and 135°) directions which are induced by the twisting phase become obvious, and the OAM distributions related to the polarization topological charges are compressed toward the center, as shown in Figure 6e,f for $u = 8 \times 10^{13}$ mm^{-2}.

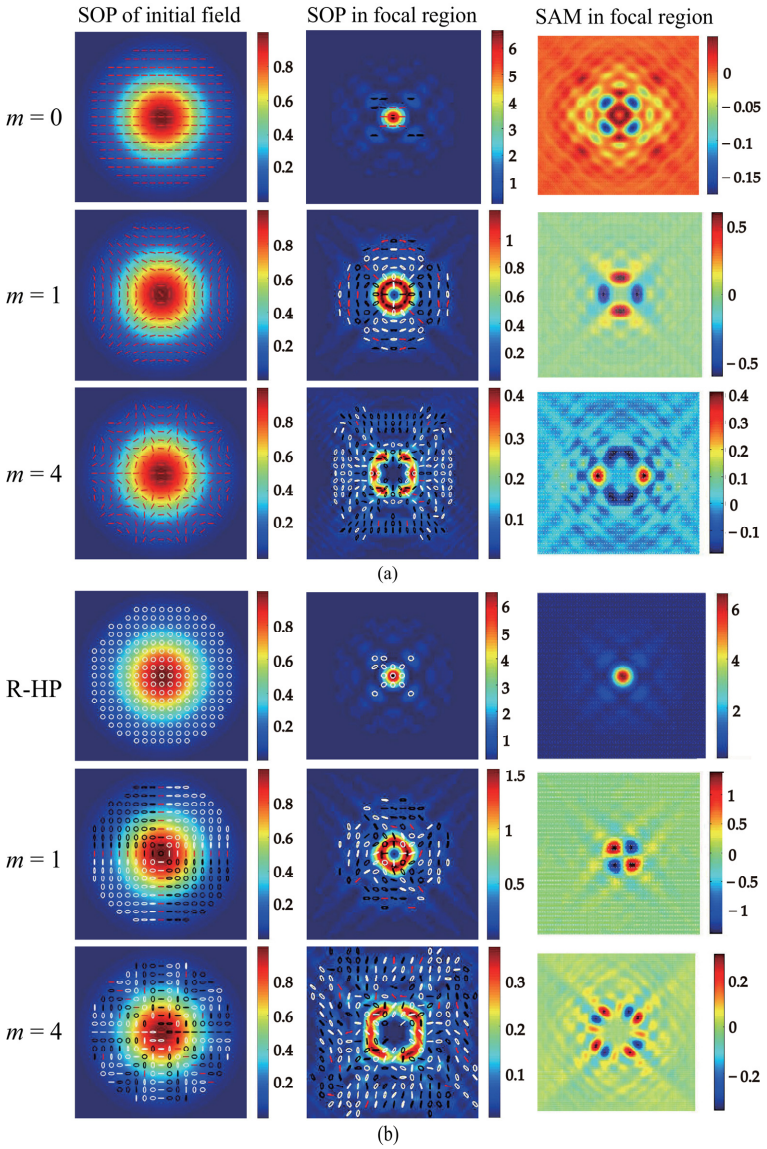

Figure 4. The SOP of scalar and vector beams in the initial field and focal region, and the corresponding SAM distribution in the focal region. The first column is the initial SOP of the input optical field, and the second and third columns are the SOP and SAM distributions with a twisting phase ($u = 10^{13}$ mm^{-2}) in the focal region: (**a**) the locally linear polarization ($\Delta\phi = 0$ in Equation (1)), (**b**) the hybrid SOP ($\Delta\phi = \pi/2$ in Equation (1)). The size of each plot in the first column is 5500λ × 5500λ, and the size of each plot in the second and third columns is 3λ × 3λ. Here the vortex topological charge $n = 0$. The red, black, and white lines indicate the linear, left-, and right-polarizations, respectively.

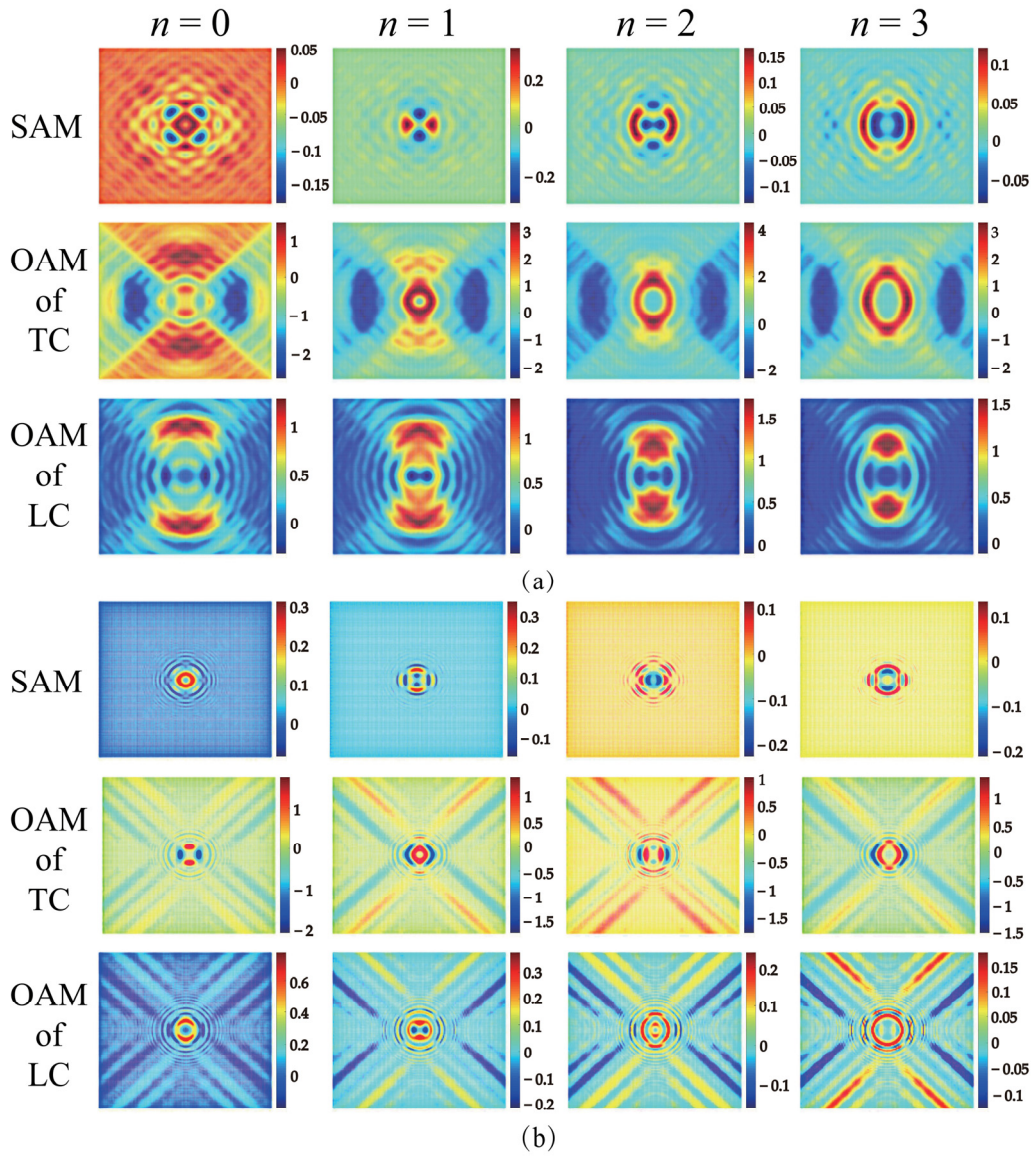

Figure 5. The SAM and OAM distributions of a focused scalar linear polarized beam (the initial field with $m = 0$ and $\phi_0 = 0$ in Equation (1)) in the focal region with different vortex topological charge numbers and the modulation of a twisting phase: (**a**) the twisted strength $u = 10^{13}$ mm^{-2}, (**b**) the twisted strength $u = 8 \times 10^{13}$ mm^{-2}. Here the size of each plot is $3\lambda \times 3\lambda$.

The SAM-OAM conversion in a focused vector vortex beam [48] and a high non-paraxial vector vortex beam [49] have been reported. The effect of a twisting phase also plays an important role in the linear–circular polarization conversion and SAM-OAM conversion of a tightly focused vector vortex beam with non-uniform SOP in the focal region. For the vector vortex beam with locally linear polarization or hybrid SOP ($\Delta\phi = 0$ or $\pi/2$ in Equation (1)) and the same topological charge number, the TC OAM distributions are similar, as shown in the first column in Figure 7. It can be explained as the OAM of two corresponding orthogonal polarization components being equal and incoherent, although the OAM is modulated by the twisting phases. However, the OAM distributions of the LC are different for the focused twisted vector beam with the same topological charge number but dissimilar SOP (locally linear polarization or hybrid SOP), as shown in the second column in Figure 7. The distinct OAM distributions of the LC can be explained by the variations in the linear–circular polarization conversions of the two SOP during the focusing, leading to the differences in the spin–orbital angular momentum transformations and OAM distributions in the LC. Thus, the effect of a twisting phase on the tightly focused

scalar and vector optical field can induce the generation and redistribution of OAM in both TC and LC, as shown in Figure 7c,d. These results provide a new way to further vectorially manipulate the structured optical field in the aspects of the optical field, SOP, and OAM via the twisting phase.

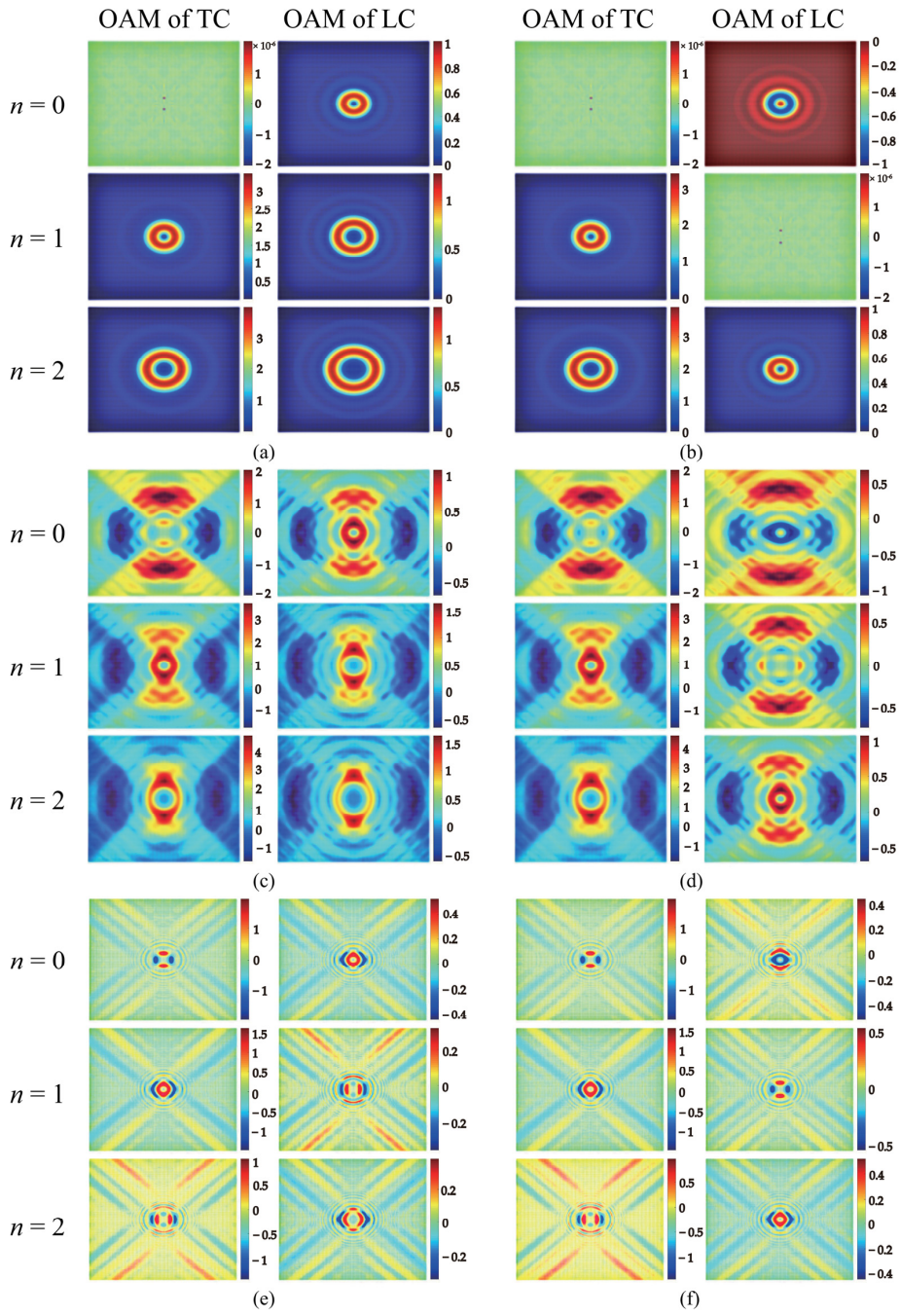

Figure 6. The OAM distribution of a focused scalar circularly polarized beam in the focal region with different vortex topological charges without (**a**,**b**) or with (**c**,**d**) the modulation of a twisting phase: (**a**) the left circularly polarized light (the initial field with $m = 0$ and $\phi_0 = \pi/4$ in Equation (1)), (**b**) the right circularly polarized light (the initial field with $m = 0$ and $\phi_0 = -\pi/4$ in Equation (1)), (**c**) the left circularly polarized light modulated by a twisting phase with $u = 10^{13}$ mm^{-2}, (**d**) the right circularly polarized light modulated by a twisting phase with $u = 10^{13}$ mm^{-2}, (**e**) the left circularly polarized light modulated by a twisting phase with $u = 8 \times 10^{13}$ mm^{-2}, (**f**) the right circularly polarized light modulated by a twisting phase with $u = 8 \times 10^{13}$ mm^{-2}. Here the size of each plot is $3\lambda \times 3\lambda$.

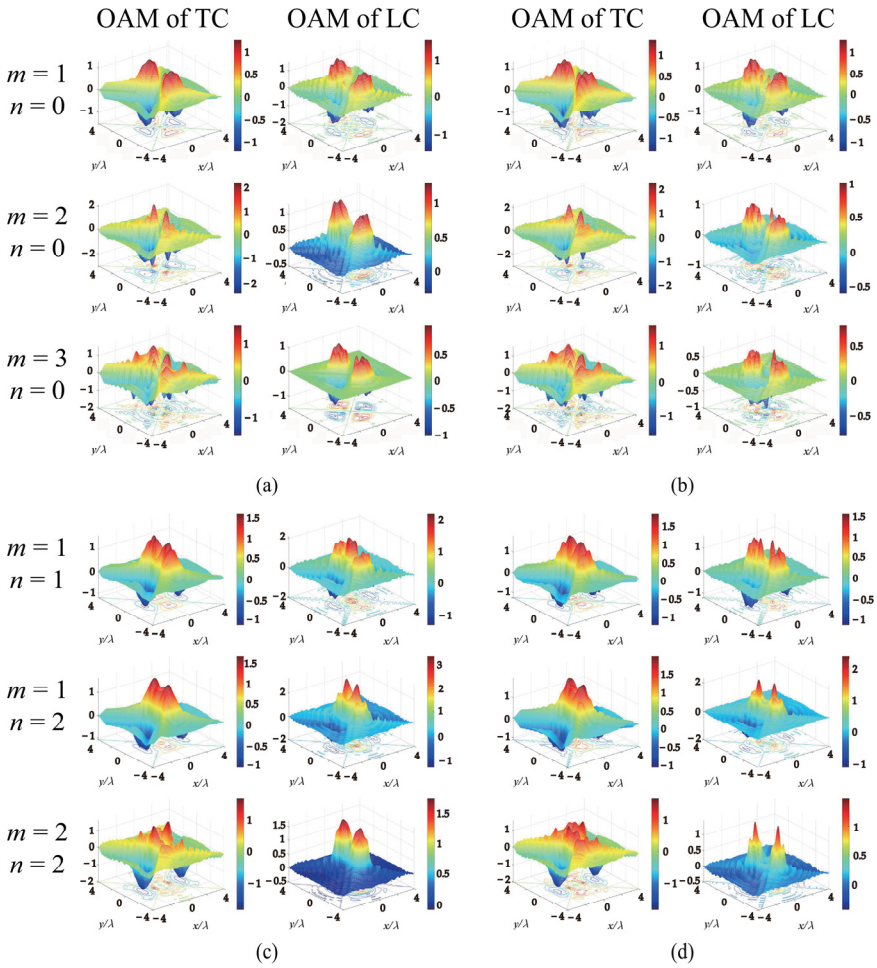

Figure 7. The OAM distribution of a focused twisted vector vortex beam in the focal region: (**a**,**c**) the locally linear polarization ($\Delta\phi = 0$ in Equation (1)); (**b**,**d**) the hybrid SOP ($\Delta\phi = \pi/2$ in Equation (1)). Here, the size of each plot is set as $4\lambda \times 4\lambda$. The initial phase is $\phi_0 = 0$ and the twisted strength is $u = 10^{13}$ mm^{-2}.

4. Discussion

The conventional non-separable quadratic twisting phase $u(x_1y_2 - x_2y_1)$ only exists in a partially coherent light field [20]. As a new type of twisting phase uxy (or $u\rho^2\cos\phi\sin\phi$ in Equation (1)) since being introduced into coherent light, some novel properties have been revealed, such as the rotation of a twisted anisotropic beam [46], measurement of vortex topological charge number [50], and the optical angular momentum resulting from the twisting phase [26]. In this work, the effect of a twisting phase on the polarization dynamics and spin–orbital angular momentum conversion of a vector vortex optical field in the focal region is studied. The results indicate that the linear–circular polarization conversion and the SAM-OAM conversion in LC occur in both scalar and vector twisted beams in the focal region due to the modulation of the twisting phase.

The underlying physics of these novel phenomena can be explained based on the non-uniform spatial phase distribution of a twisting phase uxy, which plays an essential role in the linear–circular polarization conversion during focusing. This is because the modulation and distribution of the non-uniform twisting phase uxy in the field cross-section induce a phase difference between the orthogonal polarization components in the focal region, as well as the linear–circular polarization conversion that occurs during focusing. In particular, even in a scalar optical field with a uniform linear polarization, there will be a circular polarization component (SAM) during propagation, further inducing the appearance of OAM in the LC due to the SAM-OAM conversion during tightly focusing. The OAM

of a longitudinal component in a tightly focusing beam is related to the distributions of transverse orbital and spin angular momentum, as recognized in Equation (1). In a tightly focused scalar optical field with linear polarizations, the transverse OAM is influenced by the twisting phase due to the non-uniform phase distribution of the twisting phase whereas the SAM depends on the linear–circular polarization conversion. Therefore, the longitudinal component of a tightly focused scalar optical field with linear polarizations can be manipulated by different twisting strengths u because the transverse OAM distribution and the linear–circular polarization conversion are sensitively dependent on the twisting strength of a twisting phase. These results provide a new way to manipulate the SOP and optical angular momentum.

5. Conclusions

The effect of a twisting phase on the focused scalar and vector optical field has been studied. Unlike other phase modulations, the twisting phase uxy is spatially non-uniform in distribution that results in the linear–circular polarization conversion during focusing. Since the linear–circular conversion can also occur in a scalar beam with uniform linear polarization, the conversion further induces the appearance of OAM in the LC due to the spin–orbital angular momentum transformation. The spatial distributions of the optical field, SOP, and OAM of a twisted scalar or vector beam in the focused region are sensitively dependent on the twisted strength of a twisting phase. These results provide a new way to vectorially manipulate the spatial distribution of the optical field, SOP, and OAM of a structured optical field by a twisting phase.

Author Contributions: Conceptualization, R.-P.C.; methodology, R.-P.C. and S.-D.W.; validation, R.-P.C. and K.-H.C.; investigation, S.-D.W. and R.-P.C.; data curation, S.-D.W. and R.-P.C.; supervision, R.-P.C.; writing—original draft preparation, S.-D.W.; writing—review and editing, R.-P.C. and K.-H.C. All authors have read and agreed to the published version of the manuscript.

Funding: This research was funded by the Zhejiang Provincial Key Research and Development Program (No. 2022C04007); National Natural Science Foundation of China (No. 11874323).

Institutional Review Board Statement: Not applicable.

Informed Consent Statement: Not applicable.

Data Availability Statement: Not applicable.

Conflicts of Interest: The authors declare no conflict of interest.

References

1. Youngworth, K.; Brown, T. Focusing of high numerical aperture cylindrical-vector beams. *Opt. Express* **2000**, *7*, 77–87. [CrossRef] [PubMed]
2. Zhan, Q.; Leger, J. Focus shaping using cylindrical vector beams. *Opt. Express* **2002**, *10*, 324–331. [CrossRef] [PubMed]
3. Pohl, D. Operation of a Ruby laser in the purely transverse electric mode TE01. *Appl. Phys. Lett.* **1972**, *20*, 266–267. [CrossRef]
4. Mushiake, Y.; Matsumura, K.; Nakajima, N. Generation of radially polarized optical beam mode by laser oscillation. *Proc. IEEE* **1972**, *9*, 1107–1109. [CrossRef]
5. Tidwell, S.C.; Kim, G.H.; Kimura, W.D. Efficient radially polarized laser beam generation with a double interferometer. *Appl. Opt.* **1993**, *27*, 5222. [CrossRef]
6. Dorn, R.; Quabis, S.; Leuchs, G. Sharper focus for a radially polarized light beam. *Phys. Rev. Lett.* **2003**, *23*, 233901. [CrossRef]
7. Bomzon, Z.E.; Gu, M.; Shamir, J. Angular momentum and geometrical phases in tight-focused circularly polarized plane waves. *Appl. Phys. Lett.* **2006**, *89*, 241104. [CrossRef]
8. Zhao, Y.; Edgar, J.S.; Jeffries, G.D.M.; McGloin, D.; Chiu, D.T. Spin-to-orbital angular momentum conversion in a strongly focused optical beam. *Phys. Rev. Lett.* **2007**, *7*, 73901. [CrossRef]
9. Maragò, O.M.; Jones, P.H.; Gucciardi, P.G.; Volpe, G.; Ferrari, A.C. Optical trapping and manipulation of nanostructures. *Nat. Nanotechnol.* **2013**, *8*, 807–819. [CrossRef]
10. Barreiro, J.T.; Wei, T.; Kwiat, P.G. Remote preparation of single-photon "hybrid" entangled and vector-polarization states. *Phys. Rev. Lett.* **2010**, *3*, 30407. [CrossRef]
11. Sheppard, C.J.R.; Choudhury, A. Annular pupils, radial polarization, and superresolution. *Appl. Opt.* **2004**, *43*, 4322–4327. [CrossRef] [PubMed]

12. Hao, X.; Kuang, C.; Wang, T.; Liu, X. Phase encoding for sharper focus of the azimuthally polarized beam. *Opt. Lett.* **2010**, *35*, 3928–3930. [CrossRef] [PubMed]
13. Zhan, Q. Trapping metallic Rayleigh particles with radial polarization. *Opt. Express* **2004**, *12*, 3377–3382. [CrossRef] [PubMed]
14. Zhong, M.; Gong, L.; Di, L.; Zhou, J.; Wang, Z.; Li, Y. Optical trapping of core-shell magnetic microparticles by cylindrical vector beams. *Appl. Phys. Lett.* **2014**, *105*, 181112.
15. Chen, Z.; Zeng, T.; Ding, J. Reverse engineering approach to focus shaping. *Opt. Lett.* **2016**, *41*, 1929–1932. [CrossRef] [PubMed]
16. Bialynicki-Birula, I. Local and nonlocal observables in quantum optics. *New J. Phys.* **2014**, *16*, 113056. [CrossRef]
17. Wang, H.; Wang, X.; Li, Y.; Chen, J.; Guo, C.; Ding, J. A new type of vector fields with hybrid states of polarization. *Opt. Express* **2010**, *18*, 10786. [CrossRef] [PubMed]
18. Pan, Y.; Li, Y.; Li, S.; Ren, Z.; Si, Y.; Tu, C.; Wang, H. Vector optical fields with bipolar symmetry of linear polarization. *Opt. Lett.* **2013**, *38*, 3700–3703. [CrossRef]
19. Chen, R.P.; Chen, Z.; Gao, Y.; Ding, J.; He, S. Flexible manipulation of the polarization conversions in a structured vector field in free space. *Laser Photonics Rev.* **2017**, *11*, 1700165. [CrossRef]
20. Simon, R.; Mukunda, N. Twisted Gaussian Schell-model beams. *J. Opt. Soc. Am. A* **1993**, *1*, 95. [CrossRef]
21. Friberg, A.T.; Tervonen, E.; Turunen, J. Focusing of twisted Gaussian Schell-model beams. *Opt. Commun.* **1994**, *4–6*, 127–132. [CrossRef]
22. Serna, J.; Movilla, J.M. Orbital angular momentum of partially coherent beams. *Opt. Lett.* **2001**, *26*, 405–407. [CrossRef] [PubMed]
23. Friberg, A.T.; Tervonen, E.; Turunen, J. Interpretation and experimental demonstration of twisted Gaussian Schell-model beams. *J. Opt. Soc. Am. A* **1994**, *11*, 1818. [CrossRef]
24. Ponomarenko, S.A. Twisted Gaussian Schell-model solitons. *Phys. Rev. E* **2001**, *64*, 36618. [CrossRef] [PubMed]
25. Wan, L.; Zhao, D. Controllable rotating Gaussian Schell-model beams. *Opt. Lett.* **2019**, *44*, 735–738. [CrossRef] [PubMed]
26. Liu, Z.; Wan, L.; Zhou, Y.; Zhang, Y.; Zhao, D. Progress on studies of beams carrying twist. *Photonics* **2021**, *8*, 92. [CrossRef]
27. Chen, H.; Hao, J.; Zhang, B.; Xu, J.I.; Ding, J.; Wang, H. Generation of vector beam with space-variant distribution of both polarization and phase. *Opt. Lett.* **2011**, *36*, 3179–3181. [CrossRef]
28. Chen, R.P.; Chen, Z.; Chew, K.H.; Li, P.G.; Yu, Z.; Ding, J.; He, S. Structured caustic vector vortex optical field: Manipulating optical angular momentum flux and polarization rotation. *Sci. Rep.* **2015**, *5*, 10628. [CrossRef]
29. Richards, B.; Wolf, E. Electromagnetic diffraction in optical systems. II. Structure of the image field in an aplanatic system. *Proc. R. Soc. Lond. Ser. A* **1959**, *1274*, 358–379.
30. Huang, K.; Shi, P.; Cao, G.W.; Li, K.; Zhang, X.B.; Li, Y.P. Vetor-vortex Bessel-Gauss beam and their tightly focusing properties. *Opt. Lett.* **2011**, *36*, 888–890. [CrossRef]
31. Dai, X.; Li, Y.; Liu, L. Tight focusing properties of hybrid-order Poincaré sphere beams. *Opt. Commun.* **2018**, *426*, 46–53. [CrossRef]
32. Berry, M. Paraxial beams of spinning light. *Proc. SPIE* **1998**, *3847*, 6–11.
33. Wang, X.L.; Chen, J.; Li, Y.; Ding, J.; Guo, C.S.; Wang, H.T. Optical orbital angular momentum from the curl of polarization. *Phys. Rev. Lett.* **2010**, *25*, 253602. [CrossRef] [PubMed]
34. Bialynicki-Birula, I.; Bialynicka-Birula, Z. Canonical separation of angular momentum of light into its orbital and spin parts. *J. Opt.* **2011**, *6*, 64014. [CrossRef]
35. Padgett, M.; Bowman, R. Tweezers with a twist. *Nat. Photonics* **2011**, *5*, 343–348. [CrossRef]
36. Liu, J.; Li, Z. Controlled mechanical motions of microparticles in optical tweezers. *Micromachines* **2018**, *9*, 232. [CrossRef]
37. Bliokh, K.Y.; Alonso, M.A. Angular momenta and spin-orbit interaction of non-paraxial light in free space. *Phys. Rev. A* **2010**, *82*, 063825. [CrossRef]
38. Bliokh, K.Y.; Rodríguez-Herrera, O.; Lara, D.; Ostrovskaya, E.A.; Dainty, C. Optical nanoprobing via spin-orbit interaction of light. *Phys. Rev. Lett.* **2010**, *104*, 253601.
39. Bekshaev, A.Y. A simple analytical model of the angular momentum transformation in strongly focused light beams. *Cent. Eur. J. Phys.* **2010**, *8*, 947–960. [CrossRef]
40. Monteiro, P.B.; Neto, P.A.M.; Nussenzveig, H.M. Angular momentum of focused beams: Beyond the paraxial approximation. *Phys. Rev. A* **2009**, *79*, 033830. [CrossRef]
41. Bekshaev, A.Y.; Bliokh, K.Y.; Soskin, M. Internal flows and energy circulation in light beams. *J. Opt.* **2011**, *13*, 053001. [CrossRef]
42. Angelsky, O.V.; Bekshaev, A.Y.; Hanson, S.G.; Zenkova, C.Y.; Mokhun, I.I.; Zheng, J. Structured light: Ideas and concepts. *Front. Phys.* **2020**, *8*, 00114. [CrossRef]
43. Bliokh, K.Y.; Nori, F. Transverse and longitudinal angular momenta of light. *Phys. Rep.* **2015**, *592*, 1–38. [CrossRef]
44. Aiello, A.; Banzer, P.; Neugebauer, M.; Leuchs, G. From transverse angular momentum to photonic wheels. *Nat. Photonics* **2015**, *9*, 789–795. [CrossRef]
45. Bekshaev, A.Y. Transverse spin and the hidden vorticity of propagating light fields. *J. Opt. Soc. Am. A* **2022**, *39*, 1577–1583. [CrossRef] [PubMed]
46. Liu, Q.; Chew, K.H.; Huang, Y.; Liu, C.; Hu, X.; Li, Y.; Chen, R.P. Effect of twisting phases on the polarization dynamics of a vector optical field. *Photonics* **2022**, *9*, 722. [CrossRef]
47. Kotlyar, V.V.; Kovalev, A.A.; Nalimov, A.G. Energy density and energy flux in the focus of an optical vortex: Reverse flux of light energy. *Opt. Lett.* **2018**, *43*, 2921–2924. [CrossRef]

48. Pan, D.; Chew, K.H.; Wu, Y.; Chen, R.P. Conversions of linear-circular polarizations and spin-orbital angular momentums in a focused vector vortex beam with fractional topological charges. *Optik* **2022**, *252*, 168473. [CrossRef]
49. Chen, R.P.; Chew, K.H.; Dai, C.Q.; Zhou, G. Optical spin-to-orbital angular momentum conversion in the near field of a highly nonparaxial optical field with hybrid states of polarization. *Phys. Rev. A* **2017**, *96*, 053862. [CrossRef]
50. Shen, D.; Zhao, D. Measuring the topological charge of optical vortices with a twisting phase. *Opt. Lett.* **2019**, *44*, 2334–2337. [CrossRef]